4. R. D. Hancock, *Acc. Chem. Res.*, **23**, 253 (1990).
5. S. S. Lee, J. H. Jung, D. J. Chang, B. Y. Lee, and S. -J. Kim, *Bull. Korean Chem. Soc.*, **11**, 521 (1990).
6. R. M. Izatt, J. S. Bradshaw, S. A. Nielsen, J. D. Lamb, and J. J. Christensen, *Chem. Rev.*, **85**, 271 (1985).
7. M. H. Mazor, J. A. McCammon, and T. P. Lybrand, *J. Am. Chem. Soc.*, **111**, 55 (1989).
8. W. L. Hase, M.-C. Richou, and S. L. Mondro, *J. Phys. Chem.*, **93**, 539 (1989).
9. L. X. Dang and P. A. Kpllman, *J. Am. Chem. Soc.*, **112**, 5716 (1990).
10. A. Hofmanova, J. Koryta, M. Brezina, and M. L. Mittal, *Inorg. Chim. Acta*, **28**, 73 (1978) and references therein.
11. A. Agostiano, M. Caselli and M. D. Monica, *J. Electroanal. Chem. Interfac. Electrochem.*, **74**, 95 (1976).
12. EG and G Princeton Applied Research Application Note S-6 (1981).
13. Details were described in C. H. Lee's MS thesis, Korea University, 1991.
14. J. D. Lamb, R. M. Izatt, C. S. Swain, and J. J. Christensen, *J. Am. Chem. Soc.*, **102**, 475 (1980).
15. E. L. Yee, J. Tabib, and M. J. Weaver, *J. Electroanal. Chem. Interfac. Electrochem.*, **96**, 241 (1979).
16. S. Rodge, C. -W. Lee, C. Ng, and K. N. Raymonds, *Inorg. Chem.*, **26**, 1622 (1987).

Molecular Dynamics Study on the Structural Phase Transition of Crystalline Silver Iodide

Jun Sik Lee, Mee Kyung Song, and Mu Shik Jhon*

Department of Chemistry, and Center for Molecular Science, Korea Advanced Institute of Science and Technology, Seoul 130-650. *Received April 30, 1991*

The β to α phase transition in silver iodide is studied with the (*N, V, E*) and (*N, P, T*) molecular dynamics (MD) method. In experiments, the phase transition temperature is 420 K. Upon heating of β form, the iodine ions undergo hcp to bcc transformation and silver ions become mobile. MD simulations for the β and α phases are carried out at several temperatures and the radial distribution functions (rdf) are obtained at those temperatures in the (*N, V, E*) ensemble. But the phase transition is not found in our calculation. Next the phase transition is studied with the (*N, P, T*) MD and we find some evidences of phase transition. At 3 Kbars and 2 Kbars the phase transition temperature is about 300 K. For 3.55 Kbars, the phase transition is higher (420 K) than the low pressure case. The phase transition temperature is somewhat dependent on the pressure in our calculations.

Introduction

In the last several years, many theoretical and experimental works have been done for the study of crystalline silver iodide, which, in the high temperature α phase, may be considered as the model of the superionic conductor. Superionic conductors are a class of systems in which pheomena observed in fluids and solids come together in an interesting manner.[1-3] Silver iodide shows a number of structural transitions as a function of pressure and temperature.[4,5] At 420 K, β phase undergoes a transition into superionic α phase.

Computer simulation is one of most powerful techniques of studying liquids and highly anharmonic solids. Historically, Monte Carlo method was the first simulation technique applied to determine the equilibrium properties of fluids, such as their pair distribution functions and the thermodynamic properties.[6] This approach consists of using a canonical ensemble in which a given number of particles N are confined to fixed volume V at temperature T. Usually the particles interact with an assumed potential $\phi(r_{ij})$, where r_{ij} is the distance between particles i and j and periodic boundary conditions are used to simulate an infinite system. Other ensembles, such as the isothermal-isobaric one in which N, T, and P are fixed but the volume V fluctuates, have also been used.[7] For molecular systems, the first Monte carlo calculation was that of Barker and Watts who used the canonical (*N, V, T*) ensemble to study a model of liquid water.[8] Subsequent workers have employed the (*N, V, T*) approach and also the (*N, P, T*) ensemble to test a variety of potential models for molecular systems and such calculations are now routine. In the other simulation technique, called molecular dynamics (MD),[9] the Newtonian equations of motion are integrated numerically for the systems of N particles, confined to a fixed volume V. It was Anderson[10] who first proposed how one might carry out MD calculations under conditions of constant temperature, constant pressure, or constant temperature and pressure rather than the more usual constant energy and volume. Note that in the method of Anderson only changes in the volume of the cell were possible but not in its shape. Thus crystal structure transitions are inhibited in Anderson's method because of the suppression of the essential fluctuations, namely those in the shape of MD cell. The next important development was the work of Parrinello and Rahman[11,12] who introduced a Lagrangian that allowed for the possibility that the MD cell might changes its shape. An alternative procedure rescales the coordinates of each atom at each time step. The atomic coordinate and the characteristic distance for repeating boundary conditions are re-

Tabel 1. MD Cell Parameters for The Alpha and Beta Phase

	α	β
a (Å)	5.048	4.598
b (Å)	5.048	4.598
c (Å)	5.048	7.512
α (deg)	90	90
β (deg)	90	120
γ (deg)	90	90
Density (g/cm^3)	6.061	5.669
Space group	Im3m	P63mc

scaled respectively.[13]

First, we investigate the phase transition of crystalline silver iodide by classical (*N, V, E*) MD method at several temperatures. Next, (*N, P, T*) MD method is applied at several temperatures and pressures to compare the effect of ensemble choice on the phase transition of crystalline silver iodide. We find some evidences of the phase transition with (*N, P, T*) ensemble.

Method of Calculation

The Model System and Interatomic Potential Functions. Low-temperature β phase has the hexagonal wurtzite structure with the P63mc space group: Iodine ions form an hcp lattice and silver ions are tetrahedrally coordinated to each iodine and show no self-diffusion. The crystal structure of α phase for the highest temperature range, from 148 ℃ to the melting point 555℃, was investigated by Strock.[14] According to his X-ray study, α AgI has a cubic cell in which two silver ions are distributed statistically over forty two sites around the body centered arrangement of iodide ions. He considered that the silver atoms may behave almost liquid-like in accordance with the remarkably high ionic conductivity of this phase.[15] Our calculations are performed on a 108-particle system both for the α and β phase structures. The cell parameters for α and β phase are shown in Table 1.

We used Vashishta and Rahman's potential function.[16]

$$V_{ij}=\frac{A_{ij}(\sigma_i+\alpha_j)^n}{r^n}+\frac{Z_iZ_je^2}{r}-\frac{1}{2}(\alpha_iZ_i^2+\alpha_jZ_j^2)\frac{e^2}{r^4}-\frac{W_{ij}}{r_6} \quad (1)$$

Here, *i, j* describes the type of ions; A_{ij} the repulsive strength; α_i, α_j the particle radii; σ_i, σ_j the electronic polarizabilities. The following particle radii and electronic polarizabilities are used; $\sigma_I=2.2$ Å, $\sigma_{Ag}=0.63$ Å, $\sigma_{Ag}=0$, and $\sigma_I=6.52$. The ionic charges Z for two particles are 0.6 and $W_{AgAg}=W_{AgI}=0$, $W_{II}=6.23$. For each pair, the potential functions are as follows.

$$V_{AgAg}=\frac{H_{AgAg}}{r^{n(AgAg)}}+\frac{0.36}{r} \quad (2)$$

$$V_{AgI}=\frac{H_{AgI}}{r^{n(AgI)}}-\frac{0.36}{r}-\frac{1.1736}{r^4} \quad (3)$$

$$V_{II}=\frac{H_{II}}{r^{n(II)}}+\frac{0.36}{r}-\frac{2.3472}{r^4}-\frac{6.9331}{r^6} \quad (4)$$

here $H_{ij}=A(\sigma_i+\sigma_j)^{n(ij)}$, $A=0.010248$, with angstroms and e^2 /Å$=14.39$ eV as units. In Eq. (2) to Eq. (4), all H_{ij} and $n(ij)$ are as follows.[16]

$H_{AgAg}=0.014804$ $\quad n(AgAg)=11$

$H_{AgI}=114.48$ $\quad n(AgI)=9$

$H_{II}=446.64$ $\quad n(II)=7$

Calculational Details. In the classical (*N, V, E*) MD simulation, the particles are distributed to their X-ray positions[17,18] at the initial state of each simulation and are given Boltzmann distribution of velocities. To eliminate the end effects at the surfaces, the equations of motion are solved using the periodic boundary conditions. About 2000 time steps are used to equilibrate the system and equations of motion are integrated using Verlet's finite difference algorithm.[19] A very short time $\Delta t=1.0*10^{-15}$ sec is used in order to effectively integrate the equations of motion.[20] We used $r_c=11.0$ Å as a cutoff distance.

In the (*N, P, T*) MD simulation, we used the Berendsen different approach[13]: weak coupling to an external bath, using the principle of least local perturbation with the required global coupling. Since the coupling strength can be varied, by appropriate choosing of characteristic temperature constant and pressure constant, the effect of the coupling can be easily evaluated and controlled. Here, we briefly introduce Berendsen's method.

First, evaluate pressure scaling factor μ from tensor and kinetic energy:

$$\Xi(t)=\frac{1}{2}\sum_{i<j}R_{ij}(t)\,F_{ij}(t)^T \quad (5)$$

where $R_{ij}=R_i-R_j$ is the vector from particle i to particle j, and F_{ij} is the force on particle j due to particle i. The summation in Eq. (5) is taken only over real atoms and the row vector is denoted as transpose of a column vector.

$$E_{kin}\left(t-\frac{1}{2}\Delta t\right)=\sum_i m_i v_i\left(t-\frac{1}{2}\Delta t\right)v_i\left(t-\frac{1}{2}\Delta t\right)^T \quad (6)$$

$$P(t)=\frac{1}{3V(t)}\left[E_{kin}\left(t-\frac{1}{2}\Delta t\right)-\Xi(t)\right] \quad (7)$$

The volume $V(t)$ is the determinant of the matrix $\boldsymbol{h}$ formed by the column vectors $\boldsymbol{a}$, $\boldsymbol{b}$, $\boldsymbol{c}$ that represent the edges of the unit cell in a space-fixed Cartesian coordinate system:

$$\mu=\left\{1+\frac{\Delta t}{\tau_p}\kappa\left[P(t)-P_o\right]\right\}^{1/3} \quad (8)$$

Here, Δt is the size of the time step, τ_p is a characteristic relaxation time of the pressure, P_o is the pressure of the external constant pressure bath, and κ is the isothermal compressibility.

Second, evaluate the temperature scaling factor λ:

$$E_{kin}\left(t-\frac{1}{2}\Delta t\right)=\sum_i\frac{1}{2}m_i v_i^2\left(t-\frac{1}{2}\Delta t\right) \quad (9)$$

$$T\left(t-\frac{1}{2}\Delta t\right)=\frac{2k}{3N-M-3}E_{kin}\left(t-\frac{1}{2}\Delta t\right) \quad (10)$$

where N is the number of atoms, M the number of constraints.

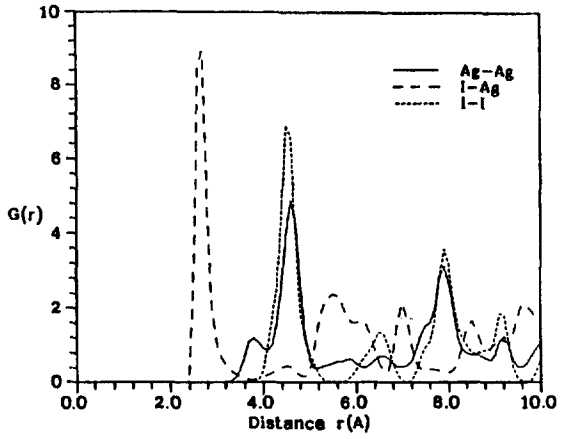

Figure 1. Radial distribution functions of β AgI at 80 K.

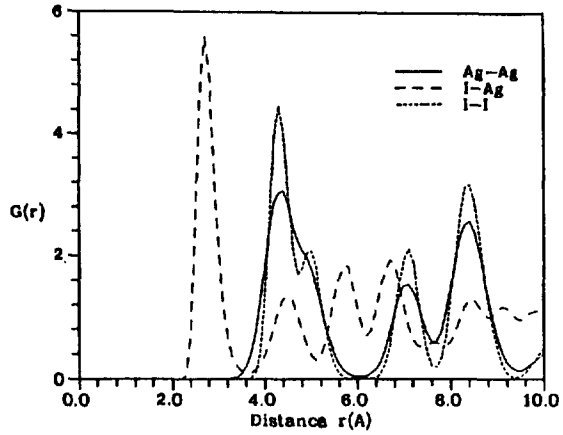

Figure 2. Radial distribution functions of α AgI at 420 K.

$$\lambda = \left[1+\frac{\Delta t}{\tau_T}\left(\frac{T_o}{T(t-\frac{1}{2}\Delta t)}-1\right)\right]^{1/2} \tag{11}$$

Here, τ_T is a characteristic relaxation time of the temperature T, T_o is the temperature of the external constant temperature bath, and $T(t-1/2\Delta t)$ is the instantaneous temperature.

Then, calculate velocities and scale them:

$$a_i(t)=\frac{F_i(t)}{m_i} \tag{12}$$

In this summation, forces of periodic images within the cutoff range are to be included.

$$v\left(t+\frac{1}{2}\Delta t\right)=v\left(t-\frac{1}{2}\Delta t\right)+a(t)\Delta t \tag{13}$$

$$v\left(t+\frac{1}{2}\Delta t\right)=\lambda v\left(t+\frac{1}{2}\Delta t\right) \tag{14}$$

Although λ is based on the temperature at $(t-1/2\Delta t)$, its value can be used to scale the velocity at $(t+1/2\Delta t)$ because of the slow variation of λ.

Calculate new coordinates and perform the pressure scaling on coordinates and cell length:

$$r(t+\Delta t)=r(t)+v\left(t+\frac{1}{2}\Delta t\right)\Delta t \tag{15}$$

Instead of scaling to coordinates, we use scaled coordinates.

Tabel 2. Coordination Numbers for I-I and Ag-I Pairs at 80, 200, and 420 K Which was Obtained by Cooling from 420 K

	80 K	200 K	420 K
$CN_{I\text{-}I}$[a]	14.01	14.01	13.99
$CN_{Ag\text{-}I}$[b]	4.00	4.01	4.01

[a,b] Coordination numbers for the I-I and Ag-I pair at 1st peak.

Tabel 3. Coordination Numbers for I-I and Ag-I Pairs at 80, 420, and 500 K Which was Obtained by Heating from 80 K

	80 K	420 K	500 K
$CN_{I\text{-}I}$[a]	12.01	11.97	12.00
$CN_{Ag\text{-}I}$[b]	4.01	4.02	4.01

[a,b] Coordination numbers for the I-I and Ag-I pair at 1st peak.

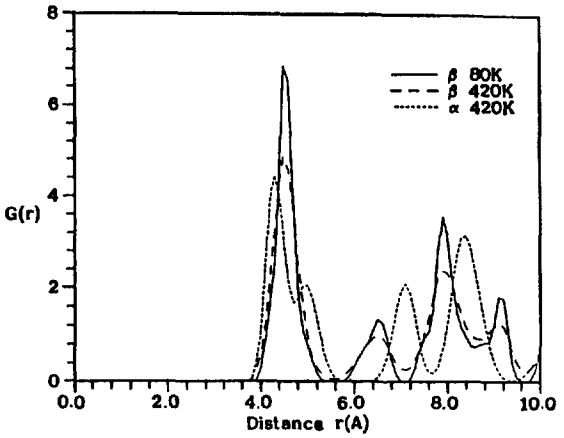

Figure 3. Radial distribution functions of β AgI at 80 and 420 K and that of α AgI at 420 K.

$$s(t+\Delta t)=h(t+\Delta t)^{-1}r(t+\Delta t) \tag{16}$$

$$h=\mu h \tag{17}$$

Now the coordinates becomes

$$r(t+\Delta t)=h(t+\Delta t)s(t+\Delta t) \tag{18}$$

In the last step, replace coordinates of particles that have moved out of the cell by the coordinates of their images within the cell. The size of time step and cutoff distance are the same with the (*N, V, E*) MD simulation. The temperature is quenched to very low temperature to obtain sharp and splitted peaks in radial distribution functions. And applied external pressures are 2, 3, and 3.55 Kbars. The characteristic relaxation times of the temperature and pressure are $\tau_T=0.01$ ps and $\tau_P=0.1$ ps, respectively.

Results and Discussion

Classical (*N, V, E*) Molecular Dynamics Study. Our calculated radial distribution functions (rdf) for β AgI at 80 K and α AgI at 420 K are the same with the crystal structures,[17,18] and they are shown in Figures 1 and 2, respectively. Ideally, for hcp (β form) and bcc (α form) structures, the $G(r)_{I\text{-}I}$ should show 6 and 4 peaks, respecively, and they are found in our calculation. It means that the classical molecular

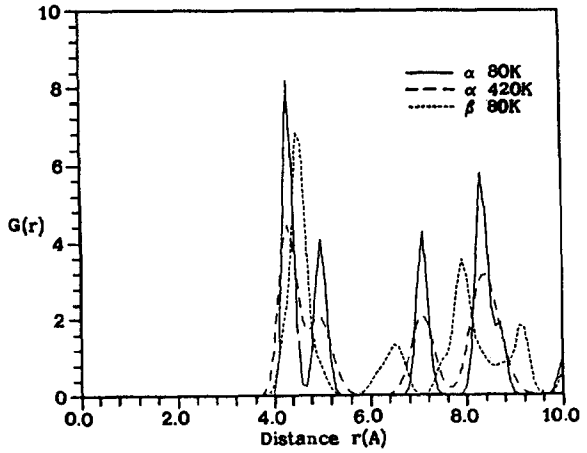

Figure 4. Radial distribution functions of α AgI at 80 and 420 K and that of β AgI at 80 K.

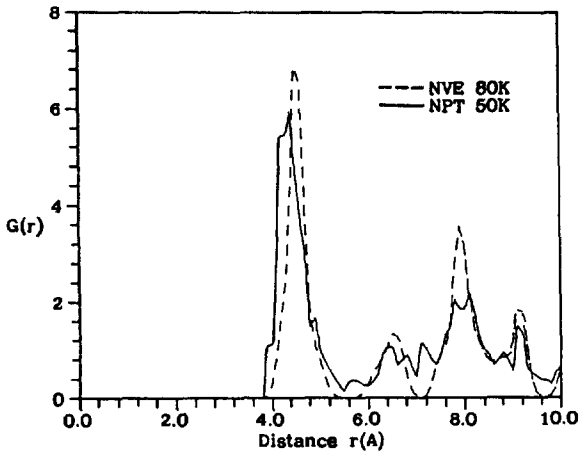

Figure 5. Radial distribution functions of I-I pair at 50 K, 3 Kbars compared with the *N, V, E* results of β phase at 80 K. The *N, P, T* result was obtained by quenching to very low temperature.

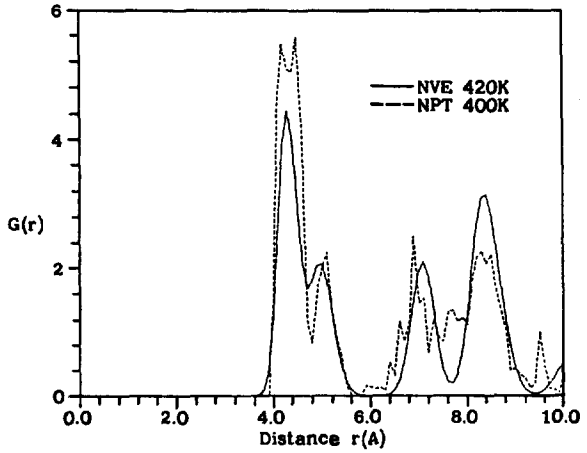

Figure 6. Radial distribution functions of I-I pair at 400 K, 3 Kbars compared with the *N, V, E* results of α phase at 420 K. The *N, P, T* result was obtained by quenching to very low temperature.

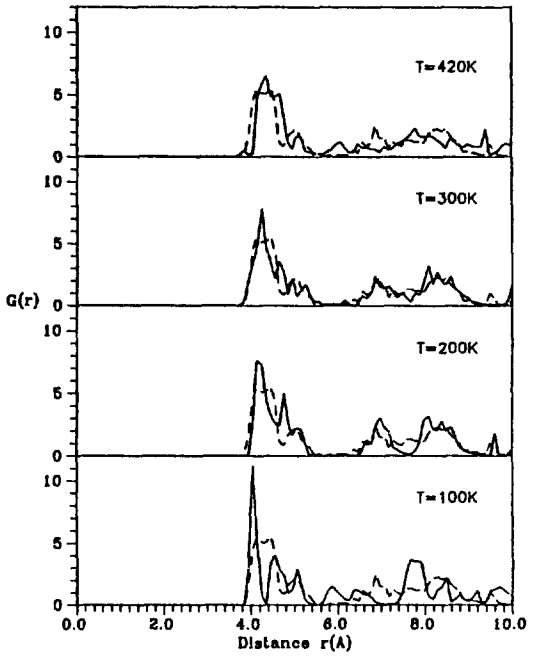

Figure 7. Radial distribution functions at 100, 200, 300, and 420 K. Each temperature was quenched to 4 K. The applied external pressure is 2 Kbars and dashed lines stand for the α phase at 400 K. Only I-I pairs are expressed.

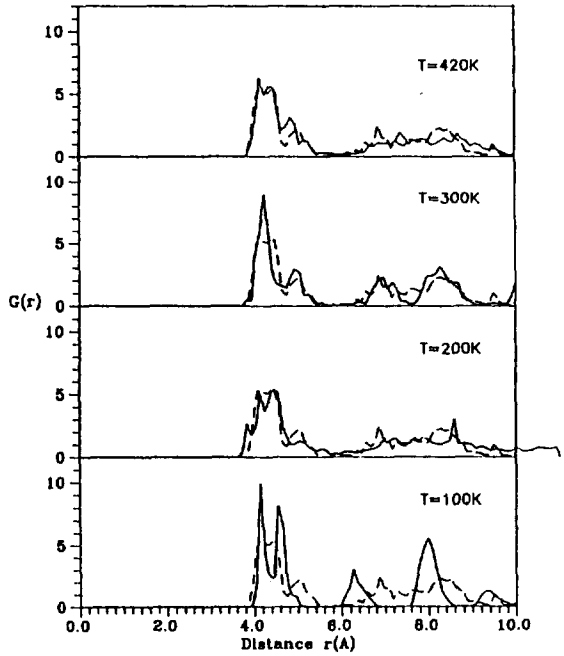

Figure 8. Radial distribution functions at 100, 200, 300, and 420 K. Each temperature was quenched to 4 K. The applied external pressure is 3 Kbars and dashed lines stand for the α phase at 400 K. Only I-I pairs are expressed.

dynamics is succeeded in maintaining each structures at given temperatures. But in the heating of β AgI from 80 to 420 K, we cannot find any changes in rdf. For cooling of α AgI, results are the same with the heating procedure except peak sharpening. Changes in coordination numbers (CN)

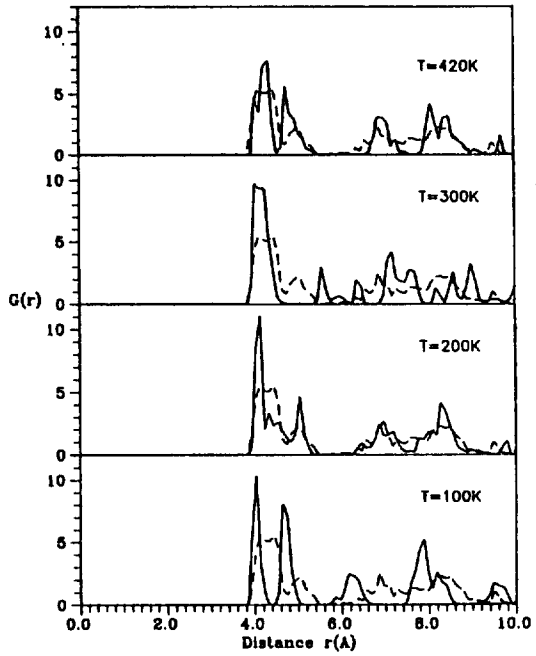

Figure 9. Radial distribution functions at 100, 200, 300, and 420 K. Each temperature was quenched to 4 K. The applied external pressure is 3.55 Kbars and dashed lines stand for the α phase at 400 K. Only I-I pairs are expressed.

with respect to the cooling of α AgI and heating of β AgI are shown in Tables 2 and 3, respectively, in which we cannot find any changes from 14 (for α AgI) to 12 (for β AgI) or 12 to 14 for CN_{I-I}. Although the temperature in heating of β AgI is high enough to experience phase transition, the changes in CN_{I-I} are not appeared. Figure 3 shows the variation of rdf, which is caused by heating β AgI from 80 to 420 K, and are compared with those of α AgI at 420 K. Figure 4 shows the variation of rdf, which is caused by cooling of α AgI from 400 to 80 K, and are compared with those of β AgI at 80 K. As can be seen in Figures 3 and 4, we cannot find any transitions except peak broadening and sharpening, respectively.

New (*N, P, T*) Molecular Dynamics Study. (*N, P, T*) MD simulations are performed at two temperatures of 50 K and 400 K at which the β and α phases exist. As we can see in Figures 5 and 6, the results of two rdf are satisfactory although they are somewhat sharper than the (*N, V, E*) results. Figure 7 shows the calculated rdf of I-I pair at each temperature for $P_o=2$ Kbar and they are compared with the results of α AgI at 400 K. The changes of rdf with respect to the peak maxima positions and shape may stand for the structural transformation. As can be seen in Figure 7, the peak shape is changed at 200 K and the transformed α phase is maintained to 300 K. The shape of the rdf at 100 K is not changed from β phase. In 200 K and 300 K, the first peak is somewhat different from α phase but the third and fourth peaks are very similar to the α phase.

For the $P^o=3$ Kbar, the result is somewhat different from $P_o=2$ Kbar case. Figure 8 shows the calculated rdf of I-I pair at each temperature and we see that α phase is appeared at 300 K. In $P_o=3.55$ Kbar, the transition is found at 420 K and results are shown in Figure 9. In all data, the splitting of first peak is the result of weak distortion of the MD cell.

Conclusions

We presented the results of MD simulations on the structural phase transition of crystalline silver iodide. The classical (*N, V, E*) MD method was failed in the phase transition study because the cell volume and shape were fixed quantifies. And then we studied transition with (*N, P, T*) MD method. In the new (*N, P, T*) method, we can find transition by fluctuating the cell volume and shape and the temperature dependence of the transition was relatively large. The phase transition temperature was proportional to the pressure. As the applied pressure increases, the phase transition temperature was also increased. The phase transition was found at 200-300 K in 2 Kbars, at 300 K, and at 420 K in 3.55 Kbars.

Acknowledgement. This work was supported in part by the Korea Science and Engineering Foundation and the Korea Research Center for Theoretical Physics and Chemistry.

References

1. *Fast Ion Transport in Solids*, edited by W. Van Gool (North-Holland, Amsterdam, 1973).
2. *Superionic Conductors*, edited by G. D. Mahan and L. R. Roth (Plenum, New York, 1976).
3. *Physics of the Superionic Conductors*, edited by M. B. Salamon (Springer-Verlag, Berlin, 1978).
4. K. Funke, *Prog. Solid State Chem.*, **11**, 345 (1976).
5. B. E. Mellander, A. Lunden, and M. Friesel, *Solid State Ionics*, **5**, 447 (1981).
6. N. Metropolis, A. W. Rosenbluth, M. N. Rosenbluth, and A. H. Teller, *J. Chem. Phys.*, **21**, 1087 (1953).
7. I. R. McDonald, *Mol. Phys.*, **23**, 42 (1972); **24**, 391 (1982).
8. A. J. Barker and R. O. Watts, *Phys. Lett.*, **3**, 144 (1969).
9. B. J. Alder and T. W. Wainright, *J. Chem. Phys.*, **27**, 1208 (1957).
10. H. C. Andersen, *J. Chem. Phys.*, **72**, 2384 (1980).
11. M. Parrinello and A. Rahman, *Phys. Rev. Lett.*, **45**, 1196 (1980).
12. M. Parrinello and A. Rahman, *J. Appl. Phys.*, **52**, 7182 (1981).
13. H. J. C. Berendsen, J. P. M. Postma, W. F. van Gunsteren, A. DiNola, and J. R. Haak, *J. Chem. Phys.*, **81**, 3684 (1984).
14. L. W. Strock, *Z. Physik. Chem.*, **B31**, 132 (1936).
15. S. Hoshino, *J. Phys. Soc. Japan*, **12**, 315 (1957).
16. M. Parrinello, A. Rahman, and P. Vashishta, *Phys. Rev. Lett.*, **50**, 1073 (1983).
17. P. R. Prager, *Prog. Cryst. Growth Charact.*, **7**, 451 (1983).
18. E. Cazzanelli, A. Fontana, G. Mariotto, F. Rocca, V. Mazzacurati, G. Ruocco, and G. Signorelli, *Phys. Rev.*, **B38**, 10883 (1988).
19. L. Verlet, *Phys. Rev.*, **159**, 98 (1967).
20. L. V. Woodcook, C. A. Angell, and P. Cheeseman, *J. Chem. Phys.*, **65**, 1565 (1976).